

# Self-consistent Skyrme QRPA for use in axially-symmetric nuclei of arbitrary mass

J. Terasaki and J. Engel

*Department of Physics and Astronomy, University of North Carolina, Chapel Hill, NC 27599-3255*

We describe a new implementation of the quasiparticle random phase approximation (QRPA) in axially-symmetric deformed nuclei with Skyrme and volume-pairing energy-density functionals. After using a variety of tests to demonstrate the accuracy of the code in  $^{24,26}\text{Mg}$  and  $^{16}\text{O}$ , we report the first fully self-consistent application of the Skyrme QRPA to a heavy deformed nucleus, calculating strength distributions for several  $K^\pi$  in  $^{172}\text{Yb}$ . We present energy-weighted sums, properties of  $\gamma$ -vibrational and low-energy  $K^\pi=0^+$  states, and the complete isovector  $E1$  strength function. The QRPA calculation reproduces the properties of the low-lying  $2^+$  states as well or better than it typically does in spherical nuclei.

PACS numbers: 21.60.Jz

Keywords: QRPA, deformed, strength function

## I. INTRODUCTION

The quasiparticle random phase approximation (QRPA) [1, 2] has a long history in nuclear physics. Its virtues include applicability to many types of excitation across the isotopic chart, preservation of energy-weighted sum rules, and elimination of spurious motion. In addition, the QRPA has several appealing interpretations; it is both a boson approximation for collective modes and the small-amplitude limit of the time-dependent Hartree-Fock-Bogoliubov (HFB) approximation. Its downside, traditionally, has been a limited ability to describe large-amplitude motion and complicated non-collective states, deficiencies that prompted the development of several more complicated methods, as, e.g., in Refs. [3, 4].

Recent years, however, have seen a revival of the QRPA, despite its drawbacks. The primary reason is the increasing connection between nuclear mean-field theory and density-functional theory (DFT) [5, 6]. The notion that Hartree-Fock or HFB calculations can be relevant beyond their naive range of validity has motivated attempts to describe a wide-range of nuclear properties in mean-field theory and extensions. The QRPA is the most straightforward extension that fits into the DFT paradigm; to the extent that the energy functional used in HFB calculations is exact, the QRPA provides the exact linear (i.e. small-amplitude) response function in the adiabatic limit [6]. Combined with its other features, its connection with DFT makes the QRPA an important tool in attempts both to develop a “Universal Nuclear Energy-Density Functional” (UNEDF), and to apply the functional to, e.g. nuclear astrophysics [7].

The prototype energy-density functional is of Skyrme form, corresponding roughly to effective interactions that have zero range, with derivatives simulating finite-range effects. In the last five or ten year, a number of groups have developed self-consistent (Q)RPA codes for use with these functionals or similar finite-range and relativistic versions, first in spherical nuclei, (see Ref. [8] and references therein), and then in axially symmetric deformed nuclei [9–13]. Heavy deformed nuclei are still problematic, however. Though the deformed RPA, without pair-

ing, is now tractable in heavy nuclei [14], a separable approximation to the Skyrme-QRPA equations has been applied in such nuclei [15, 16], and efficient new methods for solving the full QRPA equations are promising [14, 17], the numerical complexity of deformed systems has so far limited fully self-consistent Skyrme-QRPA calculations to nuclei with  $A \lesssim 40$ . In this paper, we present a highly parallelized version of the Skyrme QRPA that we are beginning to apply to heavy deformed nuclei. After discussing the structure of the code and demonstrating its accuracy, we present a preliminary application to the nucleus  $^{172}\text{Yb}$ . We focus on results here, postponing most of the formalism to a later publication.

Our QRPA code comes in several versions, developed successively as we progressed from tests in light nuclei to full-fledged calculations in heavy nuclei. All versions treat the entire Skyrme + Coulomb functional in a way that is completely consistent with HFB calculations (restricted for the time being to “volume” pairing). In addition, all the versions preserve axial and parity symmetries and the time-reversal invariance of the ground state, and therefore require an HFB code that produces single-quasiparticle wave functions of the two variables  $r \equiv \sqrt{x^2 + y^2}$  and  $z$ , with  $M \equiv \langle j_z \rangle$  a good quantum number. Finally, all diagonalize the traditional QRPA  $A, B$  matrix [1] in the “ $M$ -scheme”, and use the rigid-rotor approximation [18, 19], with the deformed QRPA solutions as intrinsic states, to calculate transition strength. The versions differ, however, in the basis in which the HFB equations are solved, in the basis in which the QRPA matrix is constructed, and in the way wave functions are represented numerically. Version a) takes quasiparticle-basis wave functions from the transformed-oscillator code HFBTHO [20] (though we use the ordinary harmonic-oscillator basis), represents the wave functions on an equidistant mesh, and constructs the QRPA matrix in the quasiparticle representation. Version b) substitutes the Vanderbilt “cylindrical-box”  $B$ -spline-based HFB code [21] for HFBTHO. Version c) modifies the QRPA part of version b) by using the canonical-quasiparticle basis, represented with  $B$ -splines, in place of the quasiparticle basis to speed calculation

and save memory. The vast majority of the computing time in all versions is in the construction of the QRPA matrix, each element of which requires a series of two-dimensional integrals for the Skyrme interaction, and an additional multipole expansion for the Coulomb interaction. The set of matrix elements can be divided among many thousands of processors so that the calculation is manageable on fast supercomputers.

Section II below describes tests in relatively light systems. Section III presents an application to heavy nuclei.

## II. TESTS

To display the accuracy of our codes, we show the results of several tests in nuclei with  $A < 40$ . We start with spurious states. A fully self-consistent and numerically perfect QRPA will completely separate spurious states from physical ones, and put them at zero energy. Small numerical errors can spoil the treatment of spurious states, however, so any calculation that separates them well has passed a serious test.

Figure 1 shows transition matrix elements of the number operators,

$$S_k^\tau = |\langle 0 | \hat{N}_\tau | k \rangle|^2, \quad (1)$$

with  $k$  labeling excitations and  $\tau$  protons/neutrons, to states with  $K^\pi = 0^+$  in a calculation of  $^{26}\text{Mg}$ . To obtain the QRPA wave functions, we use version a) of our code with the Skyrme interaction SkP [22], restricting ourselves to three harmonic oscillator shells. The HFB calculation yields pairing gaps of  $\Delta_p = 1.681$  MeV (protons),  $\Delta_n = 1.426$  MeV (neutrons) and no quadrupole deformation in this small single-particle space. This result does not imply that a calculation in a larger space also gives  $\beta = 0$  [23]. We use a small space to allow a complete QRPA treatment of two-quasiparticle excitations; a full separation of the spurious  $J^\pi = 0^+$  strength associated with the particle-number violation requires no less. And we indeed achieve essentially perfect separation. The figure shows negligible strength to all excitations except the two spurious states, which come out at  $E = 0.008$  MeV and  $0.024$  MeV.

Next, we turn to spurious rotation, arising in the  $K^\pi = 1^+$  channel. Here the nucleus must be deformed. Our HFB solution, again with SkP but for  $^{24}\text{Mg}$  in five oscillator shells, yields  $\beta = 0.28$ ,  $\Delta_p = 0.034$  MeV, and  $\Delta_n = 0.131$  MeV. Figure 2 displays the resulting transition strengths for the operator  $J_{-1} \equiv J_x - iJ_y$ . Most of the strengths are four order of magnitude smaller than that of the spurious state at  $E = 0.045$  MeV.

Finally, we examine spurious translational motion. Here, an oscillator basis for HFB is not optimal, and so we employ versions b) and c) of our code (they give identical strength functions), which use wave functions in a large cylindrical box. For these calculations, in  $^{26}\text{Mg}$ , we choose the box to have size  $r_{\text{max}} = z_{\text{max}} = 10$  fm and use the Skyrme functional SLy4 [24]. We take a

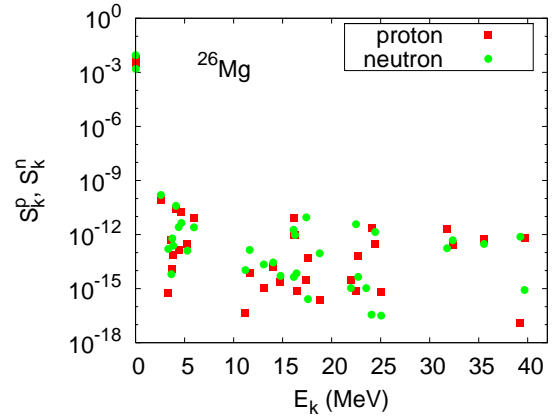


FIG. 1: (Color online) Transition strength for the proton and neutron number operators to  $K^\pi = 0^+$  states in  $^{26}\text{Mg}$  with the Skyrme functional SkP (see text).

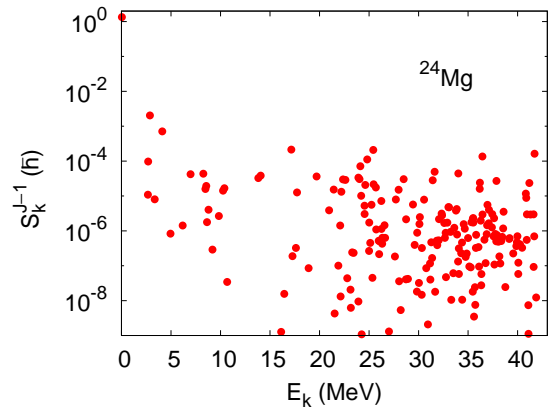


FIG. 2: (Color online) Transition strength for the operator  $J_{-1}$  to  $K^\pi = 1^+$  states in  $^{24}\text{Mg}$  with SkP.

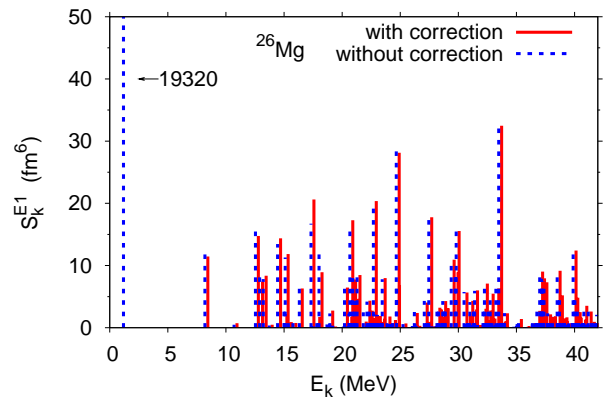


FIG. 3: (Color online) IS  $E1$  transition strength to  $K^\pi = 0^-$  states in  $^{26}\text{Mg}$  with SLy4. Solid lines represent strength that is corrected to eliminate residual spurious contributions.

TABLE I: Comparison of energies and (corrected) IS  $E1$  strengths for the three lowest-lying  $J^\pi = 1^-$  states in  $^{16}\text{O}$ , calculated with spherical ( $J$ -scheme) code and the current ( $M$ -scheme) code and SLy4. The correction barely changes the strength for the two physical excited states, but reduces that of the spurious (lowest) state by many orders of magnitude.

$J$ -scheme, $J^\pi = 1^-$		$M$ -scheme, $K^\pi = 0^-$	
$E$ (MeV)	$S_{\text{cor}}^{\text{ISE1}}$ (fm <sup>6</sup> )	$E$ (MeV)	$S_{\text{cor}}^{\text{ISE1}}$ (fm <sup>6</sup> )
0.323	$7.051 \times 10^{-5}$	0.472	$1.298 \times 10^{-4}$
7.500	$1.461 \times 10$	7.440	$1.433 \times 10$
10.610	$5.739 \times 10^{-2}$	10.681	$4.283 \times 10^{-2}$

pairing strength  $V = -140.348 \text{ MeV fm}^3$  and include quasiparticle states with energy  $\leq 300 \text{ MeV}$  in the density and pairing tensor. These parameters yield  $\beta = -0.27$ ,  $\Delta_p = 1.365 \text{ MeV}$ , and  $\Delta_n = 0.002 \text{ MeV}$ . Figure 3 shows isoscalar (IS)  $E1$  transition strengths, for which the excitation operator is  $\sum_{i=1}^A r_i^3 Y_{1\mu}(\Omega_i)$ , to states with  $K^\pi = 0^-$ . The figure contains two sets of lines, the second of which adds a correction term to the IS operator (via the prescription of Ref. [12]) to remove residual spurious strength from physical excitations. The difference between the two sets is very small in all the physical states shown, and completely negligible in higher-energy states. In sum, our code is accurate enough to handle spurious states in this mass region extremely well.

Since we have done extensive calculations with a spherical  $J$ -scheme code over the past few years [25], we can test our current codes further by comparing their results with those obtained in the  $J$  scheme. Table I shows energies and IS  $E1$  transition strengths (with the correction mentioned above) for the three lowest  $J^\pi = 1^-$  levels, along with the corresponding  $K^\pi = 0^-$  energies and strengths from version b) of our current code, in the spherical nucleus  $^{16}\text{O}$ . The two codes take wave functions from entirely different HFB codes: a slightly modified version of HFBRAD [22] called HFBMARIO for the spherical QRPA and the Vanderbilt HFB code for the deformed QRPA. The first state on each side of the table is the spurious state, with very small strength because of the correction. The next two, both genuine excitations, are nearly the same in both energy and strength in the two calculations. The full strength function, folded with a Lorentzian of width 3 MeV (see in Eq. (1) in Ref. [8]) displayed in Fig. 4, shows the same level of agreement. The very small differences in the continuum are due to differing box boundary conditions: the spherical calculation is in a spherical box with radius 20 fm and the deformed calculation is in the same cylindrical box we used for  $^{26}\text{Mg}$ .

Before moving to heavy nuclei, we display the results of one more test — this time simultaneously checking the Vanderbilt HFB code [21] underlying our deformed

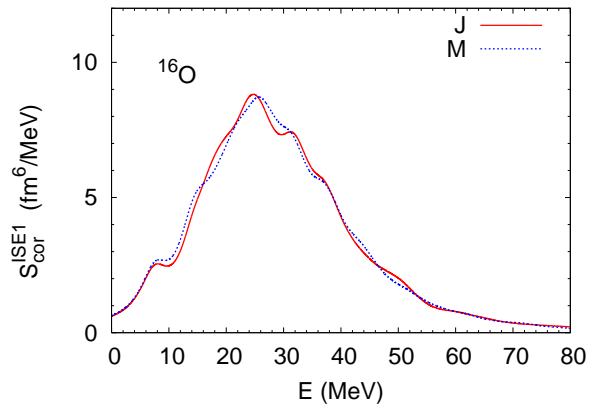


FIG. 4: (Color online) Full IS  $E1$  strength function corresponding to Tab. I. The letters J and (M) denotes the  $J$ - ( $M$ -) scheme calculations.

QRPA, and our procedure for constructing the canonical basis by diagonalizing the density matrix (which is the same as in Ref. [8]). Figure 5 displays the proton  $0p_{3/2}$  canonical basis wave function in  $^{22}\text{O}$  produced by both the spherical and deformed procedures. The agreement is perfect and far from trivial. Though  $\Delta_p = 0$  in this calculation, we still construct the density matrix from the Vanderbilt-HFB output and diagonalize it to obtain the deformed canonical wave function. (There is no arbitrariness in this wave function because only one proton  $p_{3/2}$  state is occupied in Oxygen.) The other bound-state wave functions produced by the two procedures, though we don't display them, agree equally well.

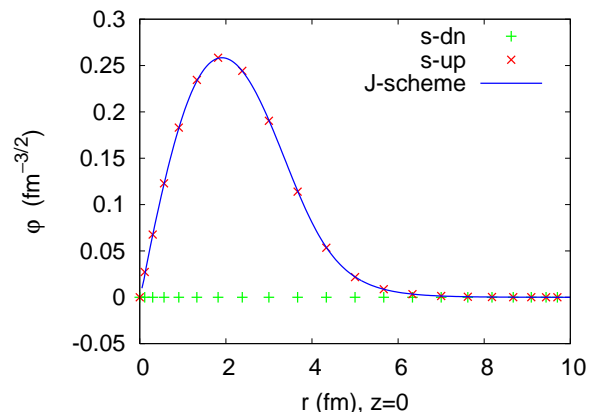


FIG. 5: (Color online) Comparison of proton  $0p_{3/2}$  canonical-basis wave function produced by  $J$ - and  $M$ -scheme codes for  $^{22}\text{O}$  at  $z = 0$ . The labels s-dn and s-up denote the spin-down and spin-up components in the  $M$ -scheme calculation. In the  $J$  scheme, the spin-down component is identically zero.

TABLE II: Energy-weighted sums for strength functions, in our QRPA calculations and from analytical sum-rule expressions. We include QRPA states with up to 90 MeV of excitation energy. The units of the IS  $E1$  sum are MeV fm<sup>6</sup>, and those of the isovector (IV)  $E1$  sum are MeV fm<sup>2</sup>. Those of all  $E2$  sums are MeV fm<sup>4</sup>. The IS  $E1$  strength has been corrected to remove spurious components. The contribution from negative values of  $K$  is not included.

Transition operator	$K^\pi$ of solution	QRPA	Analytical
IS $E1$	$1^-$	1043560	1042413
IV $E1$	$1^-$	289.819	285.764
IS $E1$	$0^-$	2015266	2019465
IV $E1$	$0^-$	291.859	285.764
IS $E2$	$2^+$	64700	63877
IV $E2$	$2^+$	20284	20076
IS $E2$	$1^+$	76159	88197
IV $E2$	$1^+$	28517	28174
IS $E2$	$0^+$	97886	96867
IV $E2$	$0^+$	31271	30874

### III. HEAVY NUCLEI

Having thoroughly tested several versions of the deformed QRPA, we apply version c), representing the best combination of speed and accuracy, to the nucleus  $^{172}\text{Yb}$ . We set up the HFB calculation as follows: we use a “box” with  $r_{\text{max}} = z_{\text{max}} = 20$  fm, cut off the quasiparticle spectrum at 60 MeV and take the maximum  $z$ -component of quasiparticle angular momentum to be 19/2; these parameters define a single-quasiparticle space with 4648 proton states and 5348 neutron states. We use the Skyrme functional SkM\* [26] with volume pairing strengths  $V_p = -218.521$  MeV fm<sup>3</sup> and  $V_n = -176.364$  MeV fm<sup>3</sup> (determined from measured odd-even mass differences). The calculation yields  $\Delta_p = 1.248$  MeV,  $\Delta_n = 0.773$  MeV, and  $\beta = 0.34$ .

We input half the canonical wave functions, those with  $j_z > 0$ , in the QRPA, and construct and truncate two-canonical-quasiparticle configurations in the following way: We define critical particle-particle and particle-hole occupation probabilities  $(v_{\text{cut}}^{\text{pp}})^2 = 10^{-6}$  and  $(v_{\text{cut}}^{\text{ph}})^2 = 10^{-10}$ . If both canonical states have occupation probabilities  $v_i^2$  and  $v_j^2$  such that  $v_i^2, v_j^2 > 1 - (v_{\text{cut}}^{\text{pp}})^2$  or  $v_i^2, v_j^2 < (v_{\text{cut}}^{\text{pp}})^2$ , we omit the configuration. We also omit configurations with  $v_i^2 < v_j^2$  for which  $v_i^2/v_j^2 < (v_{\text{cut}}^{\text{ph}})^2$ . These cuts result in a QRPA matrix whose size, while depending on multipolarity, is typically about 160,000 by 160,000.

Table II shows energy-weighted sums, alongside values obtained from sum rules, for IS and isovector (IV) electric operators in all  $^{172}\text{Yb}$  channels that we calculate. The differences between the QRPA sums and the sum rules are less than about 2% except in the IS  $K^\pi = 1^+$  channel,

TABLE III: Energies and  $B(E2; 0^+ \rightarrow 2^+)$ ’s for the  $\gamma$ -vibrational and “ $\beta$ -vib” states of  $^{172}\text{Yb}$ . Experimental data are from Ref. [27] (see also [28]). For the definition of  $B(E2)$ , see, e.g., Ref. [29].

		Exp.	Cal.
$\gamma$ -vib.	$E$ (MeV)	1.466	2.261
	$B(E2)$ ( $e^2\text{b}^2$ )	0.0433 +5–15	0.041
“ $\beta$ -vib.”	$E$ (MeV)	1.117	1.390
	$B(E2)$ ( $e^2\text{b}^2$ )	0.0081 17	0.00495

where we were unable to adequately separate the spurious rotational state without going to a larger space. In other channels the spurious mode is under better control. In the IS  $0^-$  and  $1^-$  channels, we have some contamination at low energies, but it is weak enough that the subtraction procedure of Ref. [12] restores the sum rule nearly exactly. In the  $0^+$  channel, as the table shows, the separation is quite good even without subtraction. The  $1^+$  channel can be corrected as well, but doing so requires a numerical procedure that we have not yet implemented.

The accuracy of the energy-weighted sums in the  $K^\pi = 0^+$  and  $2^+$  channels indicates that our approach is reliable for low-lying quadrupole shape vibrations. Table III shows the energies and  $B(E2; 0^+ \rightarrow 2^+)$ ’s of both the  $\gamma$ -vibrational  $K^\pi = 2^+$  state and a low-energy  $K^\pi = 0^+$  state with a significant  $B(E2)$  that we denote by “ $\beta$ -vib”. The quotation marks indicate that, unlike the clearcut  $\gamma$ -vibrational state, the  $0^+$  state has a somewhat smaller  $B(E2)$  than is typical of vibrational modes. Both states have been studied experimentally, e.g. in Ref. [27].

The agreement of both the energies of these states and their transition strengths with measured values is at a level that is typical of QRPA calculations in spherical nuclei. In Ref. [30] we investigated a large set of such nuclei, characterizing the quality of the QRPA by two quantities:

$$R_E \equiv \ln(E_{\text{cal}}/E_{\text{exp}}), \quad (2)$$

$$R_Q \equiv \ln \sqrt{B(E2)_{\text{cal}}/B(E2)_{\text{exp}}},$$

where suffices cal and exp denote calculated and experimental. The results in Tab. III correspond to  $R_E = 0.43$  and  $R_Q = -0.03$  for the  $\gamma$ -vibration, and  $R_E = 0.22$  and  $R_Q = -0.25$  for “ $\beta$ -vib.” The histograms in Figs. 4 and 9 of Ref. [30] show these values to be near the most common values in spherical nuclei.

Figure 6 displays the IV  $E1$  strength function. The thick curve is the sum of strengths in all channels, and can be compared with experimental data. The peaks of the  $K^\pi = 0^-$  and  $1^-$  distributions in Fig. 6 lie at different energies, as is often the case in deformed nuclei. Though an experimental group reports a pygmy resonance at 3 – 4 MeV [31], we see no indication of one in our calculation. It has been suggested that in spherical Sn isotopes such resonances involve configurations beyond the natu-



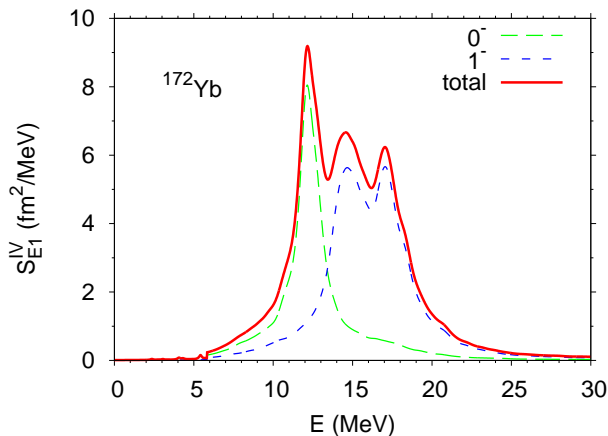


FIG. 6: (Color online) Predicted IV  $E1$  strength function in  $^{172}\text{Yb}$ , with a folding width of 0.5 MeV (0.1 MeV for discrete states).  $0^-$  and  $1^-$  indicate  $K^\pi$  components (the curve labeled  $K^\pi = 1^-$  includes the contribution of  $K^\pi = -1^-$ ).

ral ambit of the QRPA [3, 4], but the issue is unresolved, and in deformed nuclei has not been systematically investigated.

In summary, we have developed a box-based Skyrme-QRPA code for axially-symmetric even-even nuclei aimed at calculations throughout the isotopic chart. We rigorously tested the accuracy of the code in Mg isotopes,

paying particular attention to spurious states. Though the code does not do quite so well with spurious states in heavier nuclei under the restrictions on space size that we currently impose, the agreement of energy weighted sums with sum rules indicates that a) in channels with no spurious modes (e.g.  $K^\pi = 2^+$ ) our code is quite accurate, b) in the  $K^\pi = 0^+$  channel, spurious admixtures are negligible, and c) in the IS  $K^\pi = 0^-$ , and  $1^-$  channels (and the  $1^+$  channel in the future), admixtures are larger but can be effectively removed. In addition, calculations with larger spaces should be possible. Our immediate plans are to systematically investigate the ability of modern density functionals, together with the QRPA, to describe  $\beta$  and  $\gamma$  vibrations in the rare-earth nuclei.

### Acknowledgments

This work was supported by the UNEDF SciDAC Collaboration under DOE grant DE-FC02-07ER41457. We are indebted to Profs. V. E. Oberacker and A. S. Umar for giving us their HFB code and for technical support. We used computers at the National Energy Research Scientific Computing Center, the National Institute for Computational Sciences at the University of Tennessee (TeraGrid), the National Center for Computational Sciences, and the University of North Carolina at Chapel Hill.

- 
- [1] P. Ring and P. Schuck, *The Nuclear Many-Body Problem* (Springer-Verlag, New York, 1980).
  - [2] J.-P. Blaizot and G. Ripka, *Quantum Theory of Finite Systems* (MIT press, Cambridge, 1986).
  - [3] N. Tsoneva, H. Lenske, and C. Stoyanov, Phys. Lett. B **586**, 213 (2004).
  - [4] D. Sarchi, P.-F. Bortignon, and G. Colò, Phys. Lett. B **601**, 27 (2004).
  - [5] I. Z. Petkov and M. V. Stoitsov, *Nuclear Density Functional Theory* (Clarendon press, Oxford, 1991).
  - [6] C. Fiolhais, F. Nogueira, and M. Marques, eds., *A Primer in Density Functional Theory* (Springer, Berlin, 2003).
  - [7] M. Arnould and S. Goriely, Phys. Rep. **384**, 1 (2003).
  - [8] J. Terasaki, J. Engel, and M. Bender et al., Phys. Rev. C **71**, 034310 (2005).
  - [9] M. Yamagami and N. Van Giai, Phys. Rev. C **69**, 034301 (2004).
  - [10] D. Pena Arteaga and P. Ring, Phys. Rev. C **77**, 034317 (2008).
  - [11] S. Péru and H. Goutte, Phys. Rev. C **77**, 044313 (2008).
  - [12] K. Yoshida and N. Van Giai, Phys. Rev. C **78**, 064316 (2008).
  - [13] C. Losa et al. (2010), <http://arxiv.org/abs/1002.4351v1>.
  - [14] T. Inakura, T. Nakatsukasa, and K. Yabana, Phys. Rev. C **80**, 044301 (2009).
  - [15] V. O. Nesterenko et al., Phys. Rev. C **74**, 064306 (2006).
  - [16] A. P. Severyukhin et al., Phys. Rev. C **77**, 024322 (2008).
  - [17] J. Toivanen et al., Phys. Rev. C **81**, 034312 (2010).
  - [18] A. Bohr and B. R. Mottelson, *Nuclear Structure, vol. II* (Benjamin, Reading, 1975).
  - [19] V. G. Soloviev and N. Y. Shirikova, Z. Phys. **A334**, 149 (1989).
  - [20] M. V. Stoitsov et al., Comp. Phys. Comm. **167**, 43 (2005).
  - [21] A. Blazkiewicz et al., Phys. Rev. C **71**, 054321 (2005).
  - [22] J. Dobaczewski, H. Flocard, and J. Treiner, Nucl. Phys. A **422**, 103 (1984).
  - [23] M. V. Stoitsov et al., Phys. Rev. C **68**, 054312 (2003).
  - [24] E. Chabanat, P. Bonche, P. Haensel, J. Meyer, and R. Schaeffer, Nucl. Phys. A **635**, 231 (1998).
  - [25] J. Terasaki and J. Engel, Phys. Rev. C **74**, 044301 (2006).
  - [26] J. Bartel et al., Nucl. Phys. A **386**, 79 (1982).
  - [27] C. Fahlander et al., Nucl. Phys. A **541**, 157 (1992).
  - [28] <http://www.nndc.bnl.gov>.
  - [29] A. Bohr and B. R. Mottelson, *Nuclear Structure, vol. I* (Benjamin, New York, 1969).
  - [30] J. Terasaki, J. Engel, and G. F. Bertsch, Phys. Rev. C **78**, 044311 (2008).
  - [31] A. Voinov et al., Phys. Rev. C **63**, 044313 (2001).